Energy Conversion and Management 228 (2021) 113548

Contents lists available at ScienceDirect

Energy Conversion and Management

journal homepage: www.elsevier.com/locate/enconman

The value of CO_2-Bulk energy storage with wind in transmission-constrained electric power systems

Jonathan D. Ogland-Hand [a,1], Jeffrey M. Bielicki [a,b,c,*], Benjamin M. Adams [d], Ebony S. Nelson [e], Thomas A. Buscheck [f], Martin O. Saar [d,g], Ramteen Sioshansi [h]

[a] Environmental Science Graduate Program, The Ohio State University, 174 West 18th, Columbus, OH 43210, USA
[b] Department of Civil, Environmental, and Geodetic Engineering, The Ohio State University, 2070 Neil Avenue, Columbus, OH 43210, USA
[c] John Glenn College of Public Affairs, The Ohio State University, 1810 College Road, Columbus, OH 43210, USA
[d] Geothermal Energy and Geofluids Group, Department of Earth Sciences, ETH-Zurich, Sonneggstrasse 5, 8092 Zurich, Switzerland
[e] Department of Chemical and Petroleum Engineering, The University of Kansas, 1530 W. 15th, Lawrence, KS, 66045, USA
[f] Atmospheric, Earth, and Energy Division, Physical and Life Sciences Directorate, Lawrence Livermore National Laboratory, Livermore CA 94550
[g] Department of Earth and Environmental Sciences, University of Minnesota, 116 Church Street SE, Minneapolis, MN 55455, USA
[h] Department of Integrated Systems Engineering, The Ohio State University, 1971 Neil Ave., Columbus, OH 43210, USA

A R T I C L E I N F O

Keywords:
Energy storage
Carbon dioxide capture, utilization, and storage
High-voltage direct current transmission
Wind energy
Geothermal energy
Renewable energy

A B S T R A C T

High-voltage direct current (HVDC) transmission infrastructure can transmit electricity from regions with high-quality variable wind and solar resources to those with high electricity demand. In these situations, bulk energy storage (BES) could beneficially increase the utilization of HVDC transmission capacity. Here, we investigate that benefit for an emerging BES approach that uses geologically stored CO_2 and sedimentary basin geothermal resources to time-shift variable electricity production. For a realistic case study of a 1 GW wind farm in Eastern Wyoming selling electricity to Los Angeles, California (U.S.A.), our results suggest that a generic CO_2-BES design can increase the utilization of the HVDC transmission capacity, thereby increasing total revenue across combinations of electricity prices, wind conditions, and geothermal heat depletion. The CO_2-BES facility could extract geothermal heat, dispatch geothermally generated electricity, and time-shift wind-generated electricity. With CO_2-BES, total revenue always increases and the optimal HVDC transmission capacity increases in some combinations. To be profitable, the facility needs a modest \$7.78/tCO_2 to \$10.20/tCO_2, because its cost exceeds the increase in revenue. This last result highlights the need for further research to understand how to design a CO_2-BES facility that is tailored to the geologic setting and its intended role in the energy system.

1. Introduction

Emissions of greenhouse gases, such as carbon dioxide (CO_2), have increased global mean surface temperatures about 1 °C above pre-industrial temperatures, and the consequences of present and future warming are increasingly dire [1]. Stabilizing the atmospheric concentration of CO_2 emissions to mitigate the worst effects of climate change will require substantially reducing, if not eliminating, CO_2 emissions from the electricity sector, which is among the largest sources of CO_2 emissions worldwide—including about 35% of annual CO_2 emissions in the United States [1–4]. Wind turbines and solar photovoltaics can generate electricity without emitting CO_2 during operation, but high-quality resources may not be co-located with high electricity demand [5]. As a result, using high penetrations of wind and solar energy likely requires high voltage direct current (HVDC) transmission infrastructure to transmit the electricity to regions with higher electricity demand [6–8].

Wind and solar resources also vary temporally, which makes it difficult to determine the appropriate capacity of an HVDC transmission line [9]. A line that has the capacity of the wind farm or photovoltaic array will be fully utilized only a fraction of the year (e.g., in 2016, the average capacity factor for wind turbines and solar photovoltaics in the United States was 34.7% and 27.2%, respectively [10]). Absent energy storage, a smaller capacity transmission line would require curtailment

* Corresponding author at: Department of Civil, Environmental, and Geodetic Engineering, The Ohio State University, 2070 Neil Avenue, Columbus, OH 43210, USA.
E-mail address: bielicki.2@osu.edu (J.M. Bielicki).
[1] Present address: Geothermal Energy and Geofluids Group, Department of Earth Sciences, ETH-Zurich, Sonneggstrasse 5, 8092 Zurich, Switzerland.

https://doi.org/10.1016/j.enconman.2020.113548
Received 27 May 2020; Received in revised form 10 October 2020; Accepted 12 October 2020
Available online 9 December 2020

of some of the electricity that is generated. Because the cost of HVDC transmission infrastructure increases with capacity, and the revenue from electricity sales decreases with curtailment, the profit-maximizing capacity of an HVDC transmission is below the capacity of the wind farm or photovoltaic array.

Energy storage in transmission-constrained electricity systems can reduce curtailment by time-shifting variable electricity generation [11,12]. Electricity is time-shifted by storing generation in excess of HVDC transmission capacity (or of demand) and dispatching the stored energy later when generation is below transmission capacity. As a result, energy storage can increase the utilization of variable electricity capacity, the utilization of HVDC transmission capacity, and revenue. Energy storage also may increase profit-maximizing HVDC transmission capacity.

In this study, we investigate how CO_2-bulk energy storage (CO_2-BES) could operate in a realistic case study of a transmission-constrained setting in the United States. The CO_2-BES approach is based on the notion that CO_2, that is isolated from the atmosphere in deep (>800 m), porous, and permeable aquifers in sedimentary basin geothermal resources, can be circulated between the surface and subsurface to extract geothermal heat and convert it to electricity [13]. This concept is described in the literature as CO_2 Plume Geothermal [14–18]. The CO_2-BES approach implemented here also incorporates active CO_2 reservoir management, where brine is produced from the reservoir to manage reservoir overpressure from CO_2 injection and to extract geothermal heat [19–21]. While problematic leakage of buoyant CO_2 or displaced brine is unlikely [22,23], the strategic production and re-injection of brine further reduces the likelihood and consequences of leakage.

With CO_2-BES, newly captured CO_2 is geologically stored in an aquifer in a sedimentary basin geothermal resource for a priming period and continuously thereafter for the operational lifetime of the facility. During the priming period, brine is produced to the surface and strategically re-injected to control the migration of the CO_2 plume and to manage the reservoir overpressure. Once operational, the CO_2-BES facility can generate electricity on demand. This generation occurs by producing the geothermally-heated CO_2 and brine to the surface and using the energy in these fluids to generate electricity in an indirect brine organic Rankine cycle or a direct CO_2 cycle. The cooler fluids are then re-injected into the geothermal resource. The facility can also be operated for energy storage by time-shifting when the produced brine is re-injected. Here, the energy that is required to compress and inject the fluid is stored as pressure in the subsurface. Unlike other bulk energy storage technologies, namely pumped hydroelectric energy storage (PHES) and compressed air energy storage (CAES), there is a broad geospatial potential for the deployment of CO_2-BES. Sedimentary basins are ubiquitous worldwide, including approximately half of North America [24,25]. In addition, CO_2-BES can reduce CO_2 emissions directly by permanently storing the CO_2 *and* indirectly by enabling the displacement of electricity generating facilities that emit more CO_2 by technologies that emit less or no CO_2 during operation [26].

This investigation of energy storage in a transmission-constrained setting is novel in a few ways. It is the first to investigate the optimal dispatch of CO_2-BES, an emerging subsurface based energy storage approach, when used in conjunction with a variable renewable energy technology. This work also simulates the operation of CO_2-BES in finer detail than in prior work [13,26]. In addition, while prior studies investigate how PHES or CAES may affect the sizing of an HVDC transmission line [12,27], there is no similar understanding for CO_2-BES. Further, the potential of any component of the electricity system is determined in part by profitability. The current potential for energy storage in the United States is limited because market rules that regulate the functioning of the electricity grid (e.g., reserve capacity) do not compensate energy storage facilities for the full range of services they could provide [26–28]. As a result, this study is also the first to investigate the profitability of a CO_2-BES facility when operated for transmission deferral, which is a valuable application for energy storage [29,30].

2. Methods

Since profit is defined as revenue minus cost, the optimal capacity of the HVDC transmission line is a function of: total revenue from electricity sales, cost of the HVDC transmission infrastructure, and the cost of the CO_2-BES facility (if appropriate). The revenue from electricity sales and cost of the CO_2-BES facility depend on the performance of the CO_2-BES facility. As a result, and as further described in this section, to estimate profit we integrate 1) a mixed-integer linear optimization model to estimate revenue (Section 2.1); 2) a cost model to estimate the economic costs of the facility (Section 2.2); and 3) an integrated process-based model that includes a) reservoir simulations to model the injection, flow, and heat extraction of CO_2 and brine in a deep, porous, and permeable aquifer in a sedimentary basin geothermal resource and b) a coupled model of the wells and CO_2-BES facility to estimate the performance of the facility (Section 2.3).

This novel methodological integration is applied to determine the profit-maximizing capacity of an HVDC transmission line that transmits electricity hundreds of miles between a location with substantial electricity demand and a location with sedimentary-basin geothermal resources and high-quality wind resources (Section 2.4). To determine this capacity, we vary the capacity of the HVDC transmission line, in increments of 10%, from 10% (most-constrained) to 100% (least-constrained) of the assumed wind farm capacity, in the modeling and calculations. The optimal capacity of an HVDC transmission line results in the maximum total profit; the effect of CO_2-BES is determined by comparing results from which such a facility is available with those from when it is not available.

2.1. Estimated Revenue from Electricity Sales

We adapt an optimization model for CAES to estimate the revenue of a CO_2-BES facility that operates with a wind farm to sell electricity to a distant load center [12]. As is common in prior work, perfect foresight of the wind conditions and of wholesale electricity prices are assumed [12,26,31]. Furthermore, it is also assumed that the CO_2-BES facility is fully charged with twelve hours of stored energy at the beginning of the year. Here, the mixed-integer linear optimization model is briefly described; the full formulation of the model is provided in Appendix A. The objective function:

$$\max \sum_{t=1}^{T}[(1-\gamma)\chi_t p_t - (1+\gamma)\theta_t p_t] \tag{1}$$

maximizes operational profit from electricity sales over a year of operation, where χ_t is the amount of energy, in MWh, that is transmitted by the HVDC line from the wind farm and the CO_2-BES facility to the load center during hour t, θ_t is the amount of energy, in MWh, that is purchased from the load center and stored during hour t, p_t represents the hour-t wholesale electricity price, and γ represents the transmission-loss rate.

For a given transmission capacity, the revenue that is generated by the wind farm operating without CO_2-BES is estimated as:

$$\sum_{t=1}^{T}[(1-\gamma)\sigma_t p_t] \tag{2}$$

where σ_t is the amount of electricity that is generated and sold by the wind farm during hour t. This expression assumes that electricity that is generated in excess of demand is curtailed [12].

2.2. Estimated Costs of the CO_2-BES Facility and the HVDC Transmission Line

In prior work [13], costs are estimated with Geothermal Electricity Technology Evaluation Model (GETEM) [32,33]. In this work, the capital and annual operating costs are estimated in greater detail by augmenting the cost estimates from GETEM with those for geologic CO_2 storage [34] and other items (e.g., grid integration costs) [35–39]. For example, the annual costs of the CO_2-BES facility are estimated using the same approach that is used within GETEM, with additional costs for CO_2 storage (e.g., site monitoring) relevant for the CO_2 power cycle [34].

The total capital cost of the CO_2-BES facility is the sum of the estimated capital costs of the direct CO_2 cycle and of the indirect brine organic Rankine cycle. Each of those capital costs are the sum of the estimated costs to drill and equip the wells, to establish the pipelines from the production wells to the power plant and from the power plant to injection wells, of the machinery in the power plant (e.g., turbine-generator, cooling tower, pumps) and of the costs to construct it, indirect costs (e.g., project management, office work), and contingency costs. The capital cost estimates for the direct CO_2 cycle also account for CO_2 storage development costs. The grid integration capital cost is calculated for both power cycles. Section 1 of Appendix B contains more information on the cost estimates.

The cost of HVDC transmission infrastructure is drawn from prior work [7].

2.3. Estimated Performance of the CO_2-BES Facility

The performance parameters of the CO_2-BES facility that are needed for the optimization model are estimated using the same generic well pattern as in our prior work [13,26]. But rather than coupling well and power cycle models with the results of the published reservoir simulations—which (1) assume continuous production and injection of CO_2 and brine at artesian flowrates, (2) approximate the flowrates for time-shifting with energy storage from those results, (3) ignore the reservoir overpressure from priming, and (4) use generic reservoir characteristics instead of those that are specific to a particular case study—we develop a fully integrated model. Our integrated model allows us to (1) specify the injection and production well flowrates to maximize power output, (2) simulate energy storage by time-shifting fluid injection and production mass flowrates, (3) simulate the priming period and the resulting reservoir overpressure, and (4) parameterize our reservoir simulator with data that are specific to this case-study.

The injection and subsurface flow of CO_2 and brine is simulated with the Nonisothermal Unsaturated-saturated Flow and Transport (NUFT) model [40]. Some of the results for fluid properties (e.g., enthalpy, pressure, temperature) are used as the properties of the fluid as it enters the production well downhole. The wellhead properties for the production wells are determined from the well model, which are used as the inputs to the power cycle models. The properties of the fluids as they exit the power cycle models are used as the wellhead properties of the model for the injection wells. The well model and power cycle models are based on our prior work [26], and are iterated with the reservoir simulator until the temperature of the fluid exiting the injection well converges with the injection temperature that is set in the reservoir simulator. Section 2 in Appendix B provides more details on the integrated model of the CO_2-BES facility.

With this integrated model, we simulate the 30-year operation of the generic well pattern for a CO_2-BES facility, which is based on our previous work [13]. The generic well-pattern has concentric rings of fluid production wells (0.5 km radius), CO_2 injection wells (2.0 km radius), brine injection wells (2.5 km radius), and brine production wells (4.0 km radius). The CO_2-BES facility is assumed to cycle between storing energy (i.e., charging) for twelve hours and discharging energy (i.e., generating electricity) for twelve hours while continuously injecting new CO_2 at a rate of 120 kg/s (3.78 Mt/yr). This constant CO_2 injection rate increases the reservoir overpressure and we moderate the amount of brine that is re-injected during storage periods to limit this overpressure to 10 MPa [13]. The total brine-production flowrate is set to 5,000 kg/s in the priming period and in operational period, and the total CO_2 flowrate is set to 2,000 kg/s in the priming period and to 1,000 kg/s in the operational period. This CO_2 flowrate does not include the 120 kg/s of newly captured CO_2 that is constantly injected (i.e., only some of the CO_2 in the system is circulated between the surface and the subsurface). As in prior work [13], these flowrates are distributed over nine CO_2 production

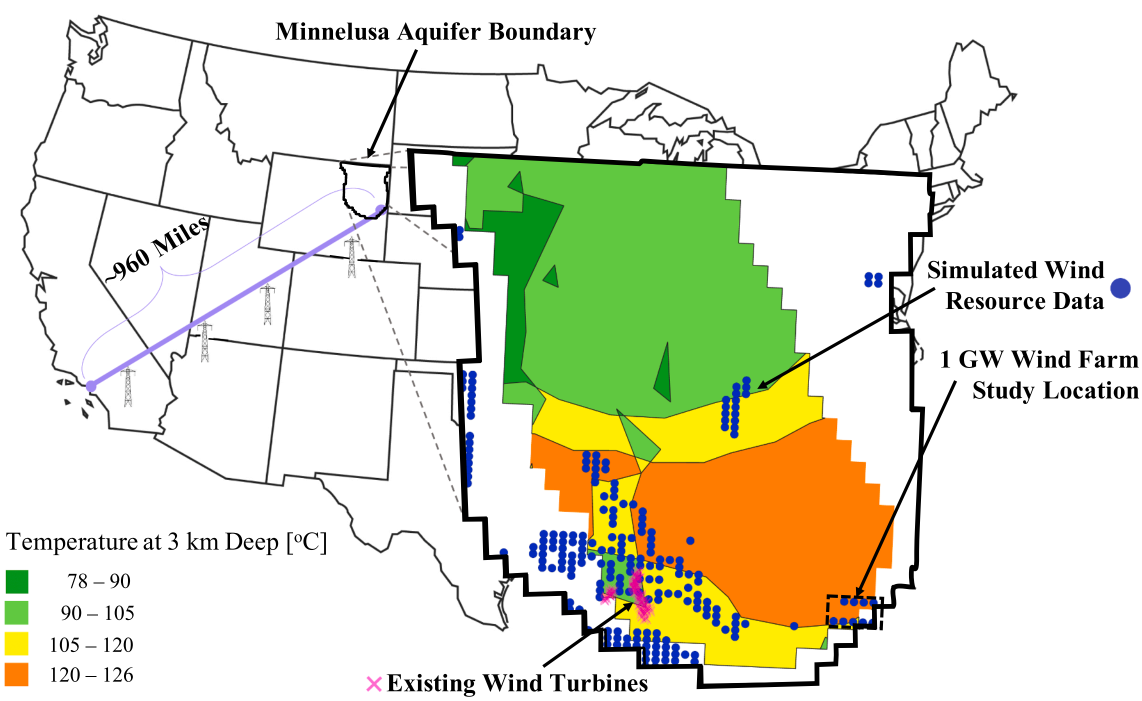

Fig. 1. High Voltage Direct Current Transmission Line Connecting the Wind Farm and CO_2-Bulk Energy Storage Facility in Eastern Wyoming to Los Angeles, California. The wind resource data (blue dots) [51], the location of existing wind turbines (pink crosses) [52], and the reservoir temperature at 3 km deep [24,42–48] are shown. (For interpretation of the references to colour in this figure legend, the reader is referred to the web version of this article.)

wells, nine CO_2 injection wells, 21 brine production wells, and 21 brine injection wells to maintain the flowrate of CO_2 below 120 kg/s per well and the flowrate of brine below 240 kg/s per well. Section 2 in Appendix B provides more details on the flowrates.

2.4. Estimated Profit and Break-Even CO_2 Price

The total profit of the wind farm with CO_2-BES is the total revenue from electricity sales as determined by the mixed-integer optimization model, less the total annualized cost of the CO_2-BES facility and the HVDC transmission infrastructure. The total profit of the wind farm without CO_2-BES is the annual electricity sales, given by (2), less the annualized cost of the HVDC transmission infrastructure. We include the cost of the HVDC transmission infrastructure because the capacity, and thus cost, may change as a result of the implementation of CO_2-BES. All capital costs are annualized with a capital recovery factor (CRF) of 11% [12].

The breakeven CO_2 price, which is the price at which CO_2-BES operators must be compensated for storing CO_2 that results in the profit using CO_2-BES equaling the profit without using CO_2-BES, is calculated as:

$$\frac{P_{withoutCO_2-BES} - P_{withCO_2-BES}}{CRF^{*}tCO_{2_{priming}} + tCO_{2_{operating}}} \tag{3}$$

where P is the profit, $tCO_{2_{priming}}$ is the amount of CO_2 that is stored permanently during the priming period, and $tCO_{2_{operating}}$ is the amount of CO_2 that is permanently stored during each year of operation. If the breakeven CO_2 price is positive, then the CO_2-BES facility would need revenue from CO_2 storage to breakeven. If the breakeven CO_2 price is negative, then using CO_2-BES increases total profit relative to a no-storage case.

2.5. Implementation of Case Study

We choose the U.S. state of Wyoming as a case study because it has substantial wind resources that are currently under-developed, favorable geothermal heat flux in the Powder River Basin (which underlies much of the state), and low electricity demand due to having a small population. Within the Powder River Basin, we use the Minnelusa Aquifer because it has properties that are favorable for geologic CO_2 storage and the operation of CO_2-BES. It is beyond the scope of this work to implement a heterogeneous reservoir model. Thus, the reservoir is assumed to be homogeneous, flat, and of constant thickness, with a permeability of 10^{-13} m^2, a porosity of 16%, a thickness of 120 m, and a depth of 2.7 km [41]. We apply a geothermal temperature gradient of 42 °C/km, which is established from a combination of North American sedimentary basin, geothermal heat flux, and CO_2 storage datasets [24,42–48]. The estimated technically accessible storage capacity of the Minnelusa Aquifer is 5,100 $MtCO_2$ [41], which is about one year of anthropogenic CO_2 emissions from the United States in 2017, or from 1,400 GW-years natural gas combined-cycle power plants [49,50]. An area that is above a portion of the Minnelusa Aquifer that has a high geothermal temperature gradient is used for a realistic 1 GW wind farm (Fig. 1).

Los Angeles, California is used as the electricity load center for a few reasons. First, Los Angeles has a high electricity demand due to its high population. Second, the U.S. state of California has aggressive policies that mandate the use of renewable energy for serving electric load. Third, an HVDC transmission line would be used to transmit electricity between Wyoming and Los Angeles. Six percent of the electricity that is transmitted over the HVDC transmission line is assumed to be lost (i.e., $\gamma = 0.06$ in (1) and (2)) [12]. Fig. 1 shows this case study.

2.5.1. Baseline Parameters

We use the most recent year (2012) of simulated wind-generated electricity in the case study area that is available from the Wind Integration National Dataset [53]. The data from 2012 is designated to be baseline data. We use 2012 wholesale electricity prices from the Vincent_2_N101 node within the system that is managed by the California Independent System Operator (CAISO) [54].

The costs of the CO_2-BES facility are estimated in 2012 U.S. dollars. The cost of HVDC transmission infrastructure [7] is converted to 2012 U.S. dollars using the producer price index adjustment factor for the Electric Bulk Power Transmission and Control Industry (Bureau of Labor Statistics Series ID PCU221121221121) [32].

2.5.2. Sensitivity Analyses

Our model estimates revenue for one year of an assumed 30-year operational lifetime. There is thus an implicit assumption that the annual performance and revenue of the CO_2-BES facility is constant. To consider sensitivity to changes in the determinants of revenue, we vary the electricity prices, wind conditions, and geothermal heat depletion as sensitivity analyses; the annual revenue from electricity depends on those three parameters and they are likely to change over the operating lifetime. We determine the optimal HVDC transmission capacity for every combination of values in the relevant parameter spaces, which are described in Sections 2.5.2.1 and 2.5.2.2.

2.5.2.1. Electricity Prices and Wind Conditions. We use historical data from 2005, as well as projections for 2024, for sensitivity analyses on electricity prices and wind conditions. Data from 2005 are obtained from the same sources that are used for the base case. Data for 2024 are from the Southern California Edison region of California and are obtained from an evaluation of California's 1,325 MW energy-storage mandate in the context of the California's renewable portfolio standard [55]. This mandate states that 50% of the electricity must come

Table 1
Mean and Standard Deviation of the Electricity Prices and Wind-Generated Electricity. The standard deviations are shown in parentheses and distributions of the data are provided in Section 3 of Appendix B.

	Wind-Generated Electricity [MWh]	Electricity Prices [$/MWh]		
2005	326.19 (329.82)		55.90 (29.46)	
2012	423.86 (337.73)		29.72 (11.59)	
			Wind and Solar Energy Penetration	
		Price Floor	33%	40%
		$0/MWh	43.77 (52.65)	39.75 (63.16)
			{44.56 (75.18)}	{41.34 (95.16)}
2024[a]	325.35 (329.39)	-$150/MWh	40.98 (47.24)	23.35 (82.80)
			{41.09 (74.01)}	{22.21 (112.97)}
		-$300/MWh	38.64 (58.70)	7.36 (121.10)
			{37.74 (85.56)}	{3.15 (144.23)}

[a] Electricity prices for 2024 [55]. Numbers refer to the results from the consideration of the energy storage mandate, unless they are in curly braces { }.

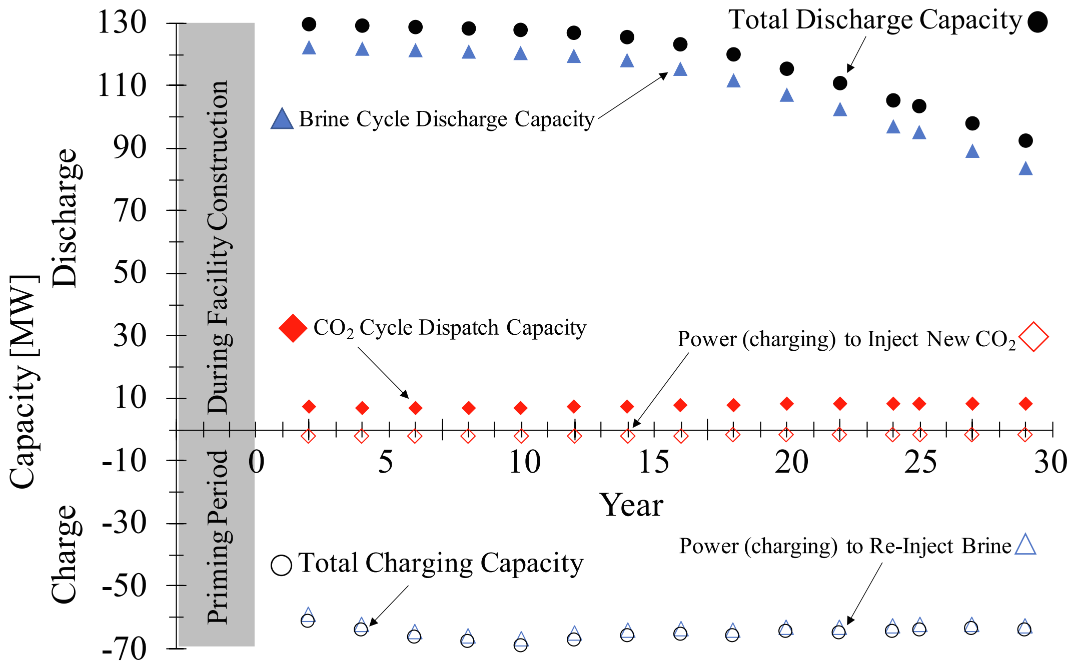

Fig. 2. Performance of the CO_2-BES Facility in Our Case Study. The facility is operated with a 12-hour charge, 12-hour discharge cycle that is repeated continuously for a lifetime of 30 years.

from qualifying renewable resources by 2030, and CAISO policy is to set negative electricity prices to avoid overgeneration by renewable generators. The study from which we draw the data examines twelve combinations of the energy storage mandate (yes or no), extent of renewable energy penetration (30% or 40%), and negative electricity prices ($0/MWh, -$150/MWh, or -$300/MWh) [55]. For wind data in 2024, we follow prior work and shift the wind data from 2005 by two days, so that the days of the week align with those in 2024 [56]. Table 1 provides summary statistics for the data sets. It shows that wind generation in 2005 and 2024 is higher than in 2012. Electricity prices are higher in 2005 than in 2012, whereas electricity prices in 2024 can be higher or lower than those in 2012, depending upon the policy conditions that are assumed.

The two wind generation datasets that are used [51,53] are available at 10-minute and 5-minute resolution, respectively. To align the wind data with the hourly electricity prices, we average the wind data across each hour.

2.5.2.2. Geothermal Heat Depletion. Because the performance of the CO_2-BES facility may change as geothermal heat is extracted, we use the simulated performance of the facility before the geothermal heat is depleted and when the heat is maximally depleted. These bounding cases of CO_2-BES performance from the first and last years of operation, respectively, are used to account for the assumption of constant annual revenue from the CO_2-BES facility.

3. Results

The degree to which the implementation of CO_2-BES increases total profits, or results in a change in the optimal HDVC transmission capacity, depends on the effect that CO_2-BES has on the utilization of wind generation and on the utilization of the HVDC transmission capacity. These effects are contingent on the performance of the CO_2-BES facility. Thus, we present the results of the integrated model of the CO_2-BES facility in Section 3.1 and the modes of operation of the CO_2-BES facility in Section 3.2. We then present the effect that CO_2-BES has on the utilization of wind generation and HVDC transmission capacity in Section 3.3, the optimal HVDC transmission capacity in Section 3.4, and the profitability of the CO_2-BES facility and break-even CO_2 prices in Section 3.5. The effects of geothermal heat depletion are presented throughout these subsections.

3.1. Performance of the CO_2-BES Facility

Over the first ten years of operation, the generic design of the CO_2-BES facility has a charging capacity between about 60 MW and 70 MW and a discharging capacity of between about 90 MW and 130 MW. Fig. 2 shows the total charging and discharging capacities of the facility over the modeled 30-year lifetime and the breakdown of these capacities between the CO_2 and brine cycles. The round-trip efficiency of the CO_2-BES facility is between 144% and 212% (92.3 MW and 64.1 MW of discharging and charging capacity, respectively, in year 30 and 129.8 MW and 61.2 MW of discharging and charging capacity, respectively, in year 2). The round-trip efficiency is greater than 100% because the geothermal heat flux added energy to the system, which can be extracted and dispatched as electricity. The round-trip efficiency decreases over the first decade of operation because of the increased charging capacity due to the reservoir overpressure from the injection of new CO_2. Over the remaining twenty years, the round-trip efficiency decreases largely because the heat in the reservoir depletes at a faster rate than it is replenished by the geothermal heat flux. This heat depletion decreases the discharging capacity. Yet, even after 30 years of operation more electricity is generated than stored and the round-trip efficiency is about 144%.

3.2. Modes of Operation of the CO_2-BES Facility

The results in Fig. 3 show that the optimization model dispatches the CO_2-BES facility in five distinct combinations of energy storage and electricity generation. These modes of operation are presented in

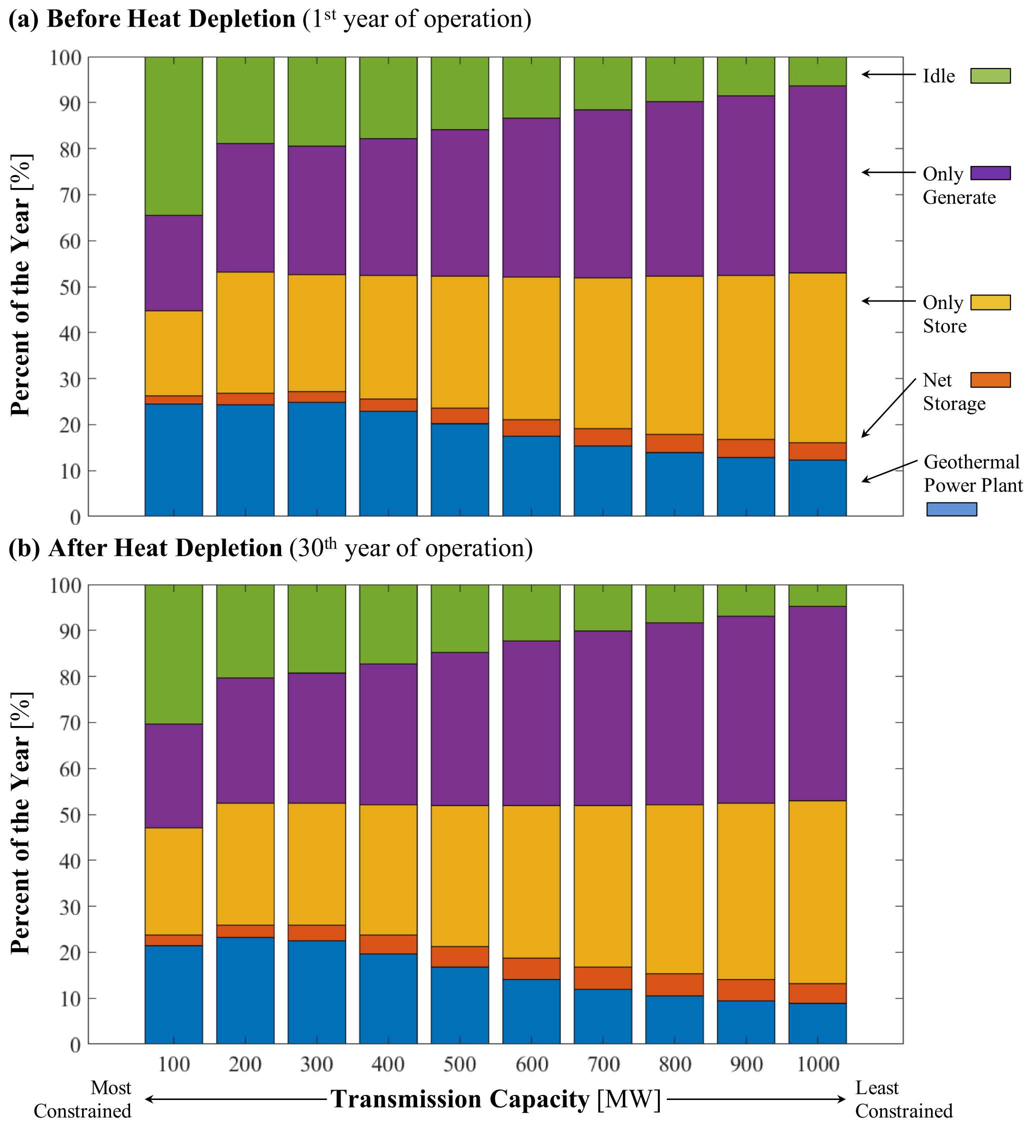

Fig. 3. Modes of Operation of the CO_2-BES Facility (a) Before Geothermal Heat Depletion (b) After 30 Years of Geothermal Heat Depletion. Values that are plotted are the average of the results for all of the combinations of wind-generated electricity and electricity prices.

Table 2
Five Modes of CO_2-BES Operation.

Mode	Description of CO_2-BES Operation	Produce Brine and CO_2?	Store Brine in Holding Pond?	Re-Inject Brine? (S)imultaneously, (HP) from Holding Pond	Re-Inject CO_2?	Inject New CO_2?
1. **Geothermal Power Plant**	Generates more electricity than the energy that it is storing simultaneously	Yes	No	S	Yes	Yes
2. **Net Energy Storage**	Stores more energy than it is generating simultaneously as electricity	Yes	No	S and HP	Yes	Yes
3. **Energy Storage Only**	Only storing electricity	No	N/A	HP	N/A	Yes
4. **Electricity Generation Only**	Only generating electricity	Yes	Yes	No	Yes	Yes
5. **Idle**	Neither is storing energy nor generating electricity	No	N/A	No	N/A	Yes

Table 2.

The amount of time the CO_2-BES facility is operated in Net Energy Storage, Energy Storage Only, and in Electricity Generation Only modes decreases with higher HVDC transmission capacities, regardless of the degree to which geothermal heat is depleted. Fig. 3(a) shows that before heat depletion, operation in the Geothermal Power Plant mode increases as transmission is less constrained until the HVDC capacity is 300 MW, beyond which the amount of time in Geothermal Power Plant mode decreases with lower transmission constraints. In contrast, Fig. 3(b) shows that after heat depletion, 200 MW of transmission capacity is the threshold beyond which the amount of time the facility operates in Geothermal Power Plant mode decreases. This reversal is a result of the

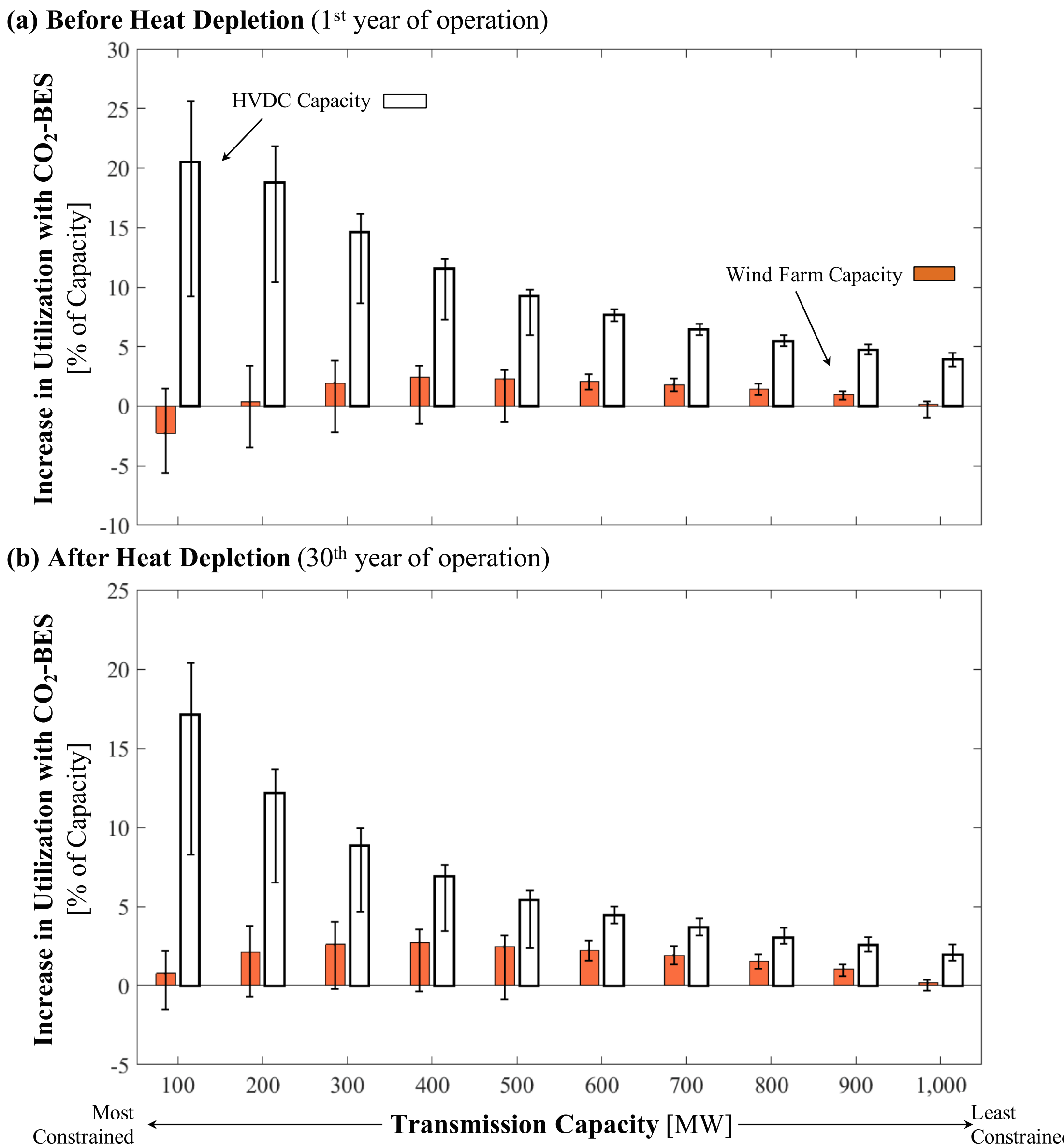

Fig. 4. Average Increase in the Utilization of HVDC Transmission Capacity and Wind-Generated Electricity Due to the Use of CO_2-BES. The error bars indicate the maximum and minimum increase across all of the 42 combinations of electricity prices and wind conditions that we investigate.

constrained maximum capacity of the CO_2-BES facility to supplement wind-generated electricity to utilize the full capacity of the transmission line. By definition, wind-generated electricity is less than the capacity of the transmission line in greater hours as the capacity of the line increases. As a result, with a higher-capacity transmission line the CO_2-BES facility is operated more frequently as a geothermal power plant to generate and transmit electricity immediately. But, the CO_2-BES facility can discharge at most about 65 MW (about 130 MW discharge less about 65 MW power consumption for pumping, before geothermal heat is depleted), which limits the potential for it to be operated as a geothermal power plant. With larger transmission capacities (400 MW in our system), it is optimal to increase the number of hours the facility operates in the other modes.

Overall, the results in Fig. 3 show that CO_2-BES has a unique capability to extract geothermal heat and dispatch it as electricity, which is optimal a non-trivial portion of the year across all of the transmission capacities that we investigate. As a consequence, the role that CO_2-BES can have in transmission-constrained systems reflects the flexibility of the technology to be used as a geothermal power plant or as an energy storage facility.

3.3. Effect of CO_2-BES on the Utilization of Wind generation and of HVDC Transmission Capacity

Fig. 4 summarizes the average increase in the utilization of HVDC transmission capacity and wind generation that result from the use of the CO_2-BES facility, across all of the combinations of electricity prices and wind conditions that we investigate (i.e., utilization rates are compared to a case without the CO_2-BES facility). The figure shows that the CO_2-BES facility has a greater effect on the utilization of the transmission as opposed to wind, and that these effects are consistent before and after the geothermal heat is depleted. For example, Fig. 4(a) shows that when transmission is most constrained, the utilization of the wind generation decreases by an average of 2.3% and the utilization of the transmission capacity increases by an average of 20.5%. Fig. 4(b) shows that after 30 years of heat depletion, the increase in the utilization of the

Table 3
Profit-Maximizing HVDC Transmission Capacity [MW]. The entries with CO_2-BES indicate the change from the optimal capacity without CO_2-BES.

Electricity Prices	Wind Conditions								
	2005			**2012**[a]			**2024**		
	w/o CO_2-BES	Δw/ CO_2-BES Heat Depletion		w/o CO_2-BES	Δw/ CO_2-BES Heat Depletion		w/o CO_2-BES	Δw/ CO_2-BES Heat Depletion	
		None	Most		None	Most		None	Most
2005[b]	700	+0	+0	800	+0	+0	700	+0	+0
2012	300	+100	+100	500	+100	+0	300	+100	+100
2024[c]	500	+100	+0	700	+100	+0	500	+0	+0
2024[d]	500	+0	+0	700	+0	+0	500	+0	+0

[a] 2012 has the windiest conditions, on average, of the three years that we consider.
[b] 2005 has the highest electricity prices, on average, of the three years that we consider.
[c] 33% renewable penetration; no energy storage mandate; $0/MWh price floor.
[d] All of the eleven other combinations.

wind generation is always positive and greater than the increase in utilization before the heat is depleted.

There are two reasons for the different trends in the utilization of transmission capacity and of wind farm capacity with CO_2-BES. First, even with transmission losses between Wyoming and Los Angeles, it can be optimal to purchase inexpensive electricity from Los Angeles, use the CO_2-BES facility to store that energy in the subsurface under Wyoming, and discharge energy to sell to Los Angeles when the price is high. This arbitrage of electricity prices increases the use of the transmission capacity but does not necessarily affect the utilization of the wind generation. Second, the geothermal heat flux provides energy that can be used to generate electricity while simultaneously storing energy in the subsurface. The additional energy from the geothermal heat flux results in a further increase in the utilization of the transmission capacity. In fact, the options to arbitrage electricity prices and to dispatch geothermal-generated electricity allow for instances in which it is profitable to curtail wind generation, especially when the transmission capacity is most constrained. This displacement of wind-generated electricity with geothermal-generated electricity occurs because revenue can be realized from the sale of geothermal-generated electricity, regardless of whether or not the wind farm generates electricity. As a result, when CO_2-BES is used in the most transmission-constrained settings, there is a decrease in the use of the wind generation and the greatest difference between the change in utilization of transmission capacity and the change in utilization of the wind farm.

3.4. Effect of CO_2-BES on the Optimal HVDC Transmission Capacity

Table 3 summarizes the optimal amounts of HVDC capacity with and without the CO_2-BES facility in cases with different wind and electricity-price conditions. For cases with the CO_2-BES facility, changes in optimal amounts of HVDC capacity relative to a case without a CO_2-BES facility are reported for the years 1 and 30 (i.e., with no and most geothermal-heat depletion). The table shows that the profit-maximizing amounts of HVDC capacity without the CO_2-BES facility range between 300 MW and 800 MW, with 500 MW being the most frequent optimal transmission capacity. Moreover, optimal HVDC capacities for a given wind condition are constant across the variations of parameters for the year 2024. This result suggests that, holding wind conditions constant, policy uncertainty surrounding the future treatment of the renewable portfolio standard and energy-storage mandate in the CAISO system should not affect using HVDC for interconnecting wind-generated electricity into California.

With CO_2-BES, the range of optimal transmission capacities narrows to be between 400 MW and 800 MW, regardless of the degree of the geothermal heat depletion. This smaller range of optimal transmission capacities occurs because it is never optimal to use a 300 MW transmission line with a CO_2-BES facility. Furthermore, the distribution of optimal transmission capacities with CO_2-BES is tighter, more bi-modal, and symmetric with equal density at 500 MW and 700 MW before the geothermal heat is depleted.

Table 4
Break-Even CO_2 Prices to Equate Profit from the Wind Farm with Additional Revenue from Geologic CO_2 Storage using CO_2-BES [\$/tCO_2]. The percentages in parenthesis are the change from the break-even CO_2 price without revenue from electricity sales (\$10.75/tCO_2).

	Before Heat Depletion	After Heat Depletion
Minimum	7.78 (−27.63%)	8.26 (–23.16%)
25th Percentile	8.73 (−18.79%)	9.20 (–14.41%)
Median	9.19 (−14.5%)	9.72 (–9.58%)
75th Percentile	9.34 (−13.12%)	9.85 (–8.37%)
Maximum	9.87 (−8.19%)	10.20 (–5.11%)

In five of the combinations of electricity prices and wind conditions, there is an increase in the optimal transmission capacity with CO_2-BES, as opposed to the two cases with geothermal heat depletion. With CO_2-BES, it is never optimal to invest in more transmission capacity in the case with the highest electricity prices (i.e., prices for the year 2005). But, in cases in which electricity prices are the lowest (i.e., prices for the year 2012), the only scenario in which inclusion of a CO_2-BES facility does not result in an increase in transmission capacity occurs after the geothermal heat is depleted with the windiest conditions.

Uncertainty in the future of the electricity system managed by the CAISO has a minor effect on optimal transmission capacity when in the presence of a CO_2-BES facility. More specifically, it is optimal to invest in more transmission capacity in one of the twelve combinations of projected electricity prices for the year 2024, which is before the geothermal heat is depleted in two of the three wind conditions.

Holding everything else constant, revenue increases with higher electricity prices and with higher amounts of wind generation. Thus, optimal transmission capacities are largest when the electricity prices are the highest and in the windiest conditions (i.e., in cases with prices from 2005 and wind conditions from 2012). As a result, if electricity is expected to be costlier, or conditions expected to be windier, larger-capacity transmission lines should be installed.

3.5. Total Profit and Break-Even CO_2 Prices

Table 4 summarizes the distribution of break-even CO_2 prices across the different wind condition and electricity price cases that we analyze. The break-even CO_2 price is \$10.75/tCO_2 when revenue from electricity sales is not included, which is the rate at which CO_2-BES operators would need to be compensated for storing CO_2 to offset the cost of the CO_2-BES facility. In this case, wind and electricity price conditions have no effect on the break-even price. When revenue from electricity sales is considered, the break-even CO_2 prices decreases by 8.19% to 27.63% (no heat depletion) or 5.11% to 23.16% (maximum heat depletion). In other words, the revenue from selling electricity across the different electricity-price, wind-condition, and heat-depeletion cases that we analyze is worth at a maximum approximately $3/t$CO_2$.

All break-even CO_2 prices are positive, which indicate that the total profit decreases when a CO_2-BES facility is built. Although CO_2-BES increases revenue, profit decreases because the cost of the CO_2-BES facility exceeds the incremental revenue from electricity sales. More specifically, the total annualized cost of the CO_2-BES facility is $167.4 million per year while the average annual increase in revenue from electricity sales with CO_2-BES ranges from $13.2 million (in the most-transmission constrained case) to $27.5 million (in the least-transmission constrained case) before geothermal heat depletion. The break-even CO_2 prices are modest and below $11/t$CO_2$ because the CO_2-BES facility stores approximately 220 MtCO_2 in the Minnelusa aquifer over the lifetime. This consists of 107 MtCO_2 over the three-year priming period and 3.8 MtCO_2/yr for the remaining 30 years of operation. Section 4 of Appendix B provides more details on the estimated costs of the CO_2-BES facility and revenue from electricity sales.

4. Discussion and Conclusions

Reducing CO_2 emissions into the atmosphere is one of the pressing challenges facing energy systems. To bridge to a cost-effective and environmentally benign energy system, the deployment and utilization of energy technologies with low and perhaps negative CO_2 emissions requires the integration of pertinent resources, systems, and infrastructure. Wind and solar energy technologies are necessary but insufficient, in part because of the temporal variability of electricity that they generate, and the potential geospatial mismatch between major electricity demand centers and high-quality wind and solar resources. Geologic storage of CO_2 is another vital component of the portfolio of approaches to mitigate climate change, and the CO_2-BES approach that we consider here isolates CO_2 in the subsurface, stores energy to time-shift variable electricity generation, and extracts geothermal heat to generate electricity.

We investigate how CO_2-BES could integrate with wind energy technologies and HVDC transmission infrastructure to address the temporal and spatial variability of wind-generated electricity to support the evolution of climate-benign energy systems. We use a realistic case study to investigate how a wind farm that is located above a sedimentary basin geothermal resource may benefit from CO_2-BES, and if CO_2-BES could increase the utilization and capacity of HVDC transmission. To do so, we simulate the operation of a CO_2-BES facility and use the process-level results in a profit maximization model to determine optimal HVDC transmission capacity and break-even CO_2 prices. As sensitivity analyses, we consider past and projected electricity prices and wind conditions and also include a bounding analysis of the performance of the CO_2-BES facility before and after 30 years of geothermal heat depletion. Even though we investigate a realistic case study in the United States, it is generalizable from the perspective that the highest quality wind resources are located in the central quarter of the contiguous United States and also overlie major sedimentary basins that are targets for geologic CO_2 storage [24,51]. The ubiquity of these basins worldwide [57], suggests that it is likely that many high-quality wind and geothermal resources are co-located [26], and that they are not necessarily located where there is high electricity demand.

As such, the broad nature of our analysis yields the following three general conclusions.

1. *Subsurface energy storage in sedimentary basin geothermal resources can operate in several modes, including as a geothermal power plant.* Consistent with our prior work [13,26,58], the geothermal energy makes it possible for the CO_2-BES facility to extract and dispatch more energy than is stored throughout its operational lifetime. As a result, the facility could be dispatched as an energy storage facility or as a geothermal power plant. It is dispatched as a geothermal power plant between one-eighth and one-quarter of the year over the various transmission constraints, degrees of geothermal heat depletion, and combinations of wind conditions and electricity prices that we investigate. We are not aware of another approach to bulk energy storage that could have a round-trip efficiency greater than 100%, or that could operate like a power plant.
2. *Subsurface energy storage in sedimentary basins could provide value in transmission-constrained electricity systems.* The use of CO_2-BES increases revenue in all of the combinations of electricity prices, wind conditions, and transmission constraints that we investigate. This increase in revenue is partly a result of the increase in the utilization of the transmission capacity by CO_2-BES time-shifting wind-generated electricity or dispatching geothermal-generated electricity.
3. *Subsurface energy storage can result in an increase in long-distance transmission capacity.* In a subset of results, and more often before geothermal heat is depleted than after 30 years of depletion, the increase in revenue with CO_2-BES is enough to increase the optimal capacity of the HVDC transmission line.

These conclusions stem from our results, which incorporate a number of assumptions in the modeling and simulations. Addressing these assumptions is beyond the scope of this work, but we present them here as three potential avenues for future work.

1. Our approach assumes that the optimal charge and discharge cycles of a CO_2-BES facility could be represented by simulations with continuous cycles of twelve hours of charging and twelve hours of discharging. This assumption follows from our prior work, which shows that a facility can be operated with flexibility as long as there are equal durations of charging and discharging energy [59]. This prior work shows also that the performance of a facility is relatively constant across different durations, so long as the discharge period is not consistently longer than the charging period. Future work could iterate between the optimization model and the CO_2-BES simulations to couple the operation of the facility and the influence on optimal transmission capacity and utilization. Another option would incorporate idle periods amidst the charging and discharging periods. These idle periods would decrease the rate of geothermal-heat depletion and the rate at which the round-trip efficiency declines. Combined, these effects should extend the usable lifetime of the CO_2-BES facility and thus increase total revenue from electricity sales.
2. Our approach couples the operation of the CO_2 power cycle and the brine power cycle, but they could be independent. For example, as long as the reservoir overpressure is between the fracture pressure of the caprock and the pressure where brine would flash as it loses pressure ascending up the production well, total revenue could increase by using the brine cycle to increase the optimal HVDC-transmission capacity and using the direct CO_2 cycle to provide high-value ancillary services. Another option could be only to build and operate the brine power cycle. The CO_2 power cycle comprises about 30% of the capital costs but provides at most about 10% of the total energy output. With this design, the CO_2 injection would be used to increase the reservoir overpressure and the charging capacity.
3. We implement a generic design of a CO_2-BES facility that is not optimized for the case study. For example, the placement of the injection and production wells does not capitalize on the permeability heterogeneity in the Minnelusa Aquifer for the best performance of the facility. Similarly, we examine a location with a relatively high estimated geothermal heat flux. Yet, the system is not designed to use this heat flow optimally. We consider a 1 GW wind farm, independent of the design of a CO_2-BES facility. Real applications should mutually consider the capacity of the energy technologies and the characteristics of their variability.

While the implementation, operation, and system integration of the CO_2-BES facility in this study are not optimized, the facility would be profitable if it is compensated modestly for geologically storing CO_2. The estimated breakeven CO_2 prices of between \$7.78/tCO_2 and \$10.20/tCO_2 are comparable with the historical CO_2 prices in California [60] and in the Regional Greenhouse Gas Initiative in the Northeast United States [61], and are below the 45Q U.S. Federal tax incentive [62] and estimates of the social cost of CO_2 [63].

Pursuing any of the following avenues for future work could also increase the revenue of the CO_2-BES facility and potentially make it profitable. For example, if the CO_2 production wells are located at the top of the reservoir to benefit from the natural buoyancy of CO_2 at reservoir conditions, the priming period and geothermal-heat depletion would decrease, which would slow the decline in discharging capacity. As such, the operational lifetime would increase, as would the total revenue. The lateral extent of the CO_2 plume would also be smaller, which would reduce costs for assessing and monitoring the Area of Review under the U.S. Environmental Protection Agency Underground Injection Control Class VI regulations. Moreover, the facility would benefit from an additional \$15/tCO_2 under the current structure of the U.S. 45Q federal tax credit [62] if the CO_2 power cycle were removed.

Because CO_2-BES can provide time-shifting energy storage services (i.e., as an energy storage facility), CO_2 storage services (as part of a CCS process), and dispatchable "firm" power (i.e., as a geothermal power plant), it is likely that CO_2-BES could provide systems-level value to the overall effort to decarbonize the electricity system [26]. In this sense, it is just as important for policy to enable the development and deployment of technologies like CO_2-BES as it is for efforts to optimize these technologies and their application. For example, policies like a renewable energy production tax credit, pricing renewable energy certificates, instituting renewable energy portfolio standards, or implementing mechanisms that put a cost on CO_2 emissions, could increase revenue for operators of CO_2-BES or other CO_2 utilization technologies even if the system design is not optimized. Uncertainty in electricity prices and wind conditions can have ramifications for under- or over-sizing the HVDC transmission line, and such policy would be beneficial to CO_2-BES operators because it would likely be more certain than the other variables that influence the value that CO_2-BES has in transmission constrained electricity systems (i.e., electricity prices and wind conditions). Such certainty can facilitate investment in climate benign technology and infrastructure, as long as it is and is robust to market fluctuations and political winds.

CRediT authorship contribution statement

Jonathan D. Ogland-Hand: Conceptualization, Methodology, Software, Validation, Formal analysis, Investigation, Data curation, Writing - original draft. **Jeffrey M. Bielicki:** Conceptualization, Methodology, Validation, Formal analysis, Investigation, Data curation, Writing - original draft, Supervision, Project administration, Funding acquisition. **Benjamin M. Adams:** Resources. **Ebony S. Nelson:** Investigation. **Thomas A. Buscheck:** Resources. **Martin O. Saar:** . **Ramteen Sioshansi:** Conceptualization, Methodology.

Declaration of Competing Interest

The authors declare that they have no known competing financial interests or personal relationships that could have appeared to influence the work reported in this paper.

Acknowledgments

The authors gratefully acknowledge funding from the U.S. National Science Foundation Innovations at the Nexus of Food, Energy, and Water Systems (INFEWS) program (1739909), National Research Traineeship Program (1922666), and SedHeat Research Coordination Network, as well as the Sustainability Institute and the Center for Energy Research Training and Innovation at The Ohio State University, the Big Ten Summer Research Opportunities Program, the Werner Siemens Foundation (Werner Siemens-Stiftung, WWS) and ETH-Zürich. We also thank Kenjiro Yagi and Dr. Paul Denholm for providing data.

Appendix A:. Full specification of the mixed integer linear optimization model

A.1 Optimization model nomenclature

We begin by defining notation for the optimization model.

A.1.1 Sets, Parameters, and Functions

T – the number of hours in the planning horizon
γ – transmission losses across the HVDC transmission line [per unit]
p_t – the price of electricity during hour t [\$/MWh], $t = 1,\ldots,T$
κ_s – the maximum amount of electricity that could be stored by the CO_2-BES facility during an hour [MWh]
κ_d – the maximum amount of electricity that could be generated by the CO_2-BES facility during an hour [MWh]
H – the maximum length of time that a CO_2-BES facility can dispatch electricity at capacity [hours]
x – the amount of electricity that is required to constantly inject external CO_2 during an hour [MWh]
G_0 – the maximum amount of energy that could be extracted from the geothermal resource over the planning horizon [MWh]
τ – the maximum amount of power that the HVDC transmission line can transmit [MW]
$\overline{w_t}$ – the amount of electricity generated by the wind farm that is available to be used during hour t [MWh], $t = 1,\ldots,T$

We model the operation of the CO_2-BES facility operating with a wind farm to sell electricity to a distant load center via an HVDC transmission line over T hourly time periods. γ measures the proportion of the electricity that is transmitted via the HVDC transmission line that is lost. A maximum of τ MW can be transmitted at any given time. When electricity is sold or purchased during hour t, the operator of the hybrid CO_2-BES and wind farm facility sells or purchases at electricity price p_t. The CO_2-BES facility operator can store a maximum amount of electricity κ_s or discharge a maximum amount of energy κ_d during any given hour period and can maintain that operation for H hours. In every time period, t, x MWh of electricity are constantly required to inject new CO_2 into the sedimentary basin geothermal resource and the wind farm can generate up to $\overline{w_t}$ MWh. Finally, a maximum of G_0 MWh of geothermal energy can be extracted and dispatched as electricity cumulatively over T.

A.1.2. Decision Variables

χ_t – the amount of electricity sold during hour t [MWh], $t = 1,\ldots,T$
θ_t – the amount of electricity purchased during hour t [MWh], $t = 1,\ldots,T$
l_t – state of energy of the CO_2-BES facility at the end of hour t [MWh], $t = 1,\ldots,T$
s_t – the amount of electricity stored by CO_2-BES facility during hour t [MWh], $t = 1,\ldots,T$
d_t – the amount of electricity dispatched by CO_2-BES facility during hour t [MWh], $t = 1,\ldots,T$
G_t – the amount of energy remaining to be extracted from the geothermal resource at the end of hour t [MWh], $t = 1,\ldots,T$
A_t – the amount of electricity that could be stored during hour t [MWh], $t = 1,\ldots,T$
w_t – the amount of electricity generated by the wind farm that is not curtailed during hour t [MWh], $t = 1,\ldots,T$
$\beta_{1,t}$ – binary variable that is 1 when the CO_2-BES and wind farm hybrid facility is purchasing electricity during hour t, $t = 1,\ldots,T$
$\beta_{2,t}$ – binary variable that is 1 when the CO_2-BES and wind farm hybrid facility is selling electricity during hour t, $t = 1,\ldots,T$

$\beta_{1,t}$ and $\beta_{2,t}$ are binary variables that represent if the hybrid facility is purchasing electricity from or selling electricity to the major load center. $\beta_{1,t} = 1$ if electricity is being purchased during hour t, and equals zero otherwise. $\beta_{2,t} = 1$ if electricity is being sold during hour t, and equals zero otherwise. χ_t represents the amount of electricity sold by the hybrid facility during hour t and θ_t represents the amount of electricity purchased by the hybrid facility during hour t. l_t represents the state of energy of the CO_2-BES facility at the end of hour t. s_t and d_t represent the amount of electricity that are stored and dispatched by the CO_2-BES facility during hour t, respectively. G_t is the ending hour-t amount of geothermal energy remaining that could be extracted during future hours. A_t represents the amount of electricity that could be stored during hour t. In other words, this variable represents the amount of brine in the surface holding pond that is available to be re-injected when the CO_2-BES operator stores electricity.

A.2. Optimization model formulation

The problem is formulated as maximizing the operational profit from net electricity sales:

$$max\sum_{t=1}^{T}[(1-\gamma)\chi_t p_t - (1+\gamma)\theta_t p_t] \tag{A1}$$

subject to:

- storage level balance:

$$l_t = l_{t-1} + \frac{\kappa_d}{\kappa_s}s_t - d_t \qquad \forall t = 1,\cdots,T \tag{A2}$$

- ability to charge:

$$A_t = A_{t-1} + \frac{\kappa_s}{\kappa_d}d_t - s_t \qquad \forall t = 1,\cdots,T \tag{A3}$$

- geothermal energy extraction:

$$G_t = G_{t-1} - \frac{G_0}{\kappa_d * H * 365}d_t \qquad \forall t = 1,\cdots,T \tag{A4}$$

- electrical energy balance:

$$\chi_t - \theta_t + s_t + x - d_t = w_t \qquad \forall t = 1,\cdots,T \tag{A5}$$

- electricity storage constraint:

$$s_t \le A_{t-1} \qquad \forall t = 1,\cdots,T \tag{A6}$$

- wind availability:

$$0 \le w_t \le \overline{w_t} \qquad \forall t = 1,\cdots,T \tag{A7}$$

- CO_2-BES facility power output capacity:

$$0 \le d_t \le \kappa_d \qquad \forall t = 1, \cdots, T \tag{A8}$$

- CO_2-BES facility energy storage capacity:

$$0 \le l_t \le H\kappa_d \qquad \forall t = 1, \cdots, T \tag{A9}$$

- CO_2-BES facility power storage capacity:

$$0 \le s_t \le \kappa_s \qquad \forall t = 1, \cdots, T \tag{A10}$$

- transmission capacity:

$$\theta_t \le \beta_{1,t}\tau \qquad \forall t = 1, \cdots, T \tag{A11}$$

$$\chi_t \le \beta_{2,t}\tau \qquad \forall t = 1, \cdots, T \tag{A12}$$

$$\beta_{1,t} + \beta_{2,t} \le 1 \qquad \forall t = 1, \cdots, T \tag{A13}$$

- non-negativity:

$$\sigma_t, \theta_t, G_t \ge 0 \qquad \forall t = 1, \cdots, T \tag{A14}$$

Objective function (A1) maximizes the operational profit from selling electricity from a location with favorable wind and sedimentary basin geothermal resources to a location with high demand. The operational profit is defined as the difference between the revenue from selling electricity to the load center and the electricity purchased from the load center. Constraints (A2) track the level of energy stored by the CO_2-BES facility, which is defined as the amount of stored energy in the previous time period plus any energy stored in the current time period less any energy dispatched. Together with Constraints (A9), they ensure that no more energy can be stored in a given time period than the CO_2-BES facility has capacity to store. Constraints (A3) tracks the brine in the holding pond at the surface that is available to be re-injected. These constraints and Constraints (A6) ensure that electricity cannot be stored via re-injecting brine if there is no brine in the holding pond to re-inject. Constraints (A4) track the total amount of geothermal energy that has yet to be extracted and used to generate electricity. These constraints along with Constraints (A14) ensure that more geothermal electricity cannot be extracted than is available to be extracted. Constraints (A5) are the electrical energy balance, which ensure that the amount of electricity sold to the distant load center, less the amount of electricity purchased, plus the amount of electricity stored by CO_2-BES, plus the electricity required to inject new CO_2, less the electricity dispatched by CO_2-BES, less the electricity generated by the wind farm, equals zero. Constraints (A7) ensure that more electricity from the wind farm cannot be generated than is available to be generated. Constraints (A8) and (A10) limit the power that is dispatched or stored in any time period to the charging and discharging capacities of the CO_2-BES facility. Constraints (A11), (A12), and (A13) together limit the amount of electricity that can be transmitted on the HVDC transmission line to the capacity of the line and also ensure that electricity can only be transmitted in one direction during any given hour, *t*.

A.1.3. Optimization model inputs that are influenced by the integrated model of CO_2-BES

We set the maximum length of time that a CO_2-BES facility can dispatch electricity at capacity (i.e., *H*) to 12 h. This is because we simulate operation of the CO_2-BES facility assuming two repeating 12-hour cycles daily in the integrated model of CO_2-BES. Although we do not simulate idle periods (i.e., periods during which electricity neither is stored nor discharged) in the integrated CO_2-BES model, it is possible that the optimal operation of CO_2-BES, as determined by the optimization model, includes idle periods throughout the year. To ensure that the electricity that is required to constantly inject CO_2 (i.e, *x*) is accounted for during idle periods, we separate it out in Constraints (A5). As a consequence, we increase the discharge capacity (K_d) and decrease the charging capacity (K_s) by the value of *x*, so that the net discharging or charging from the CO_2-BES facility is represented appropriately. For example, if the CO_2-BES facility could dispatch a maximum of 130 MWh or charge a maximum of 60 MWh, and 2 MWh were required to inject CO_2 constantly, then *x* is set to 2, K_s is set to 58, and K_d is set to 132. As a result of this separation in (A5), all of the values of *x*, K_s, and K_d are all required to define charging and discharging capacities within the optimization model for a given heat depletion scenario. We use the values that are listed in Table 5 for each heat depletion scenario that we optimize for this study.

We determine the amount of geothermal energy that is available to be extracted in a given year by using reservoir simulation results from NUFT to calculate the energy in the sedimentary basin over time. The units are converted from MJ to MWh to align with the units that are used in the optimization model. For example, the amount of energy that is available to be extracted in year one (i.e., 8,454,383.74 MWh) is the difference between the total amount of energy in the reservoir after year one and year zero.

Table 5
Optimization Model Inputs that Vary Based on Level of Geothermal Heat Depletion.

Geothermal Heat Depletion Scenario (Year)	Electricity Storage Capacity (K_s) [MWh]	Electricity Dispatch Capacity (K_d) [MWh]	Electricity Needed Inject External CO_2 (x) [MWh]	Geothermal Energy Available to be Extracted (G_0) [MWh]
No Heat Depletion (1)	59.1	131.89	2.10	8,454,383.74
High Heat Depletion (30)	62.5	93.85	1.55	5,207,435.52

Appendix B. Supplementary data

Supplementary data associated with this article can be found, in the online version, at https://doi.org/10.1016/j.enconman.2020.113548.

References

[1] IPCC. Summary for Policymakers. An IPCC Spec Rep Impacts Glob Warm 1.5 C Above Pre-Industrial Levels Relat Glob Greenh Gas Emiss Pathways. Context Strength Glob Response to Threat Clim Chang S 2018. https://www.ipcc.ch/site/assets/uploads/sites/2/2019/05/SR15_SPM_version_report_LR.pdf.

[2] Krey V, Luderer G, Clarke L, Kriegler E. Getting From Here to There – Energy Technology Transformation Pathways in the EMF27 Scenarios. Clim Change 2014:369–82. https://doi.org/10.1007/s10584-013-0947-5.

[3] Kriegler E, Weyant JP, Blanford GJ, Krey V, Clarke L, Edmonds J, et al. The Role of Technology for Achieving Climate Policy Objectives: Overview of the EMF 27 Study on Global Technology and Climate Policy Strategies. Clim Change 2014:353–67. https://doi.org/10.1007/s10584-013-0953-7.

[4] IPCC. Summary for Policymakers. Clim Chang 2014 Mitig Clim Chang Contrib Work Gr III to Fifth Assess Rep Intergov Panel Clim Chang; 2014. https://www.ipcc.ch/site/assets/uploads/2018/02/ipcc_wg3_ar5_summary-for-policymakers.pdf.

[5] U.S. DOE. 20% Wind Energy by 2030: Increasing Wind Energy's Contribution to U.S. Electricity Supply; 2008.

[6] Pleßmann G, Blechinger P. How to Meet EU GHG Emission Reduction Targets? A Model Based Decarbonization Pathway for Europe's Electricity Supply System Until 2050. Energy Strateg Rev 2017;15:19–32. https://doi.org/10.1016/j.esr.2016.11.003.

[7] MacDonald AE, Clack CTM, Alexander A, Dunbar A, Wilczak J, Xie Y. Future Cost-Competitive Electricity Systems and Their Impact on US CO2 Emissions. Nat Clim Chang 2016;6. https://doi.org/10.1038/NCLIMATE2921.

[8] Mai T, Mulcahy D, Hand MM, Baldwin SF. Envisioning a Renewable Electricity Future for the United States. Energy 2014;65:374–86. https://doi.org/10.1016/j.energy.2013.11.029.

[9] Craig MT, Cohen S, Macknick J, Draxl C, Guerra OJ, Sengupta M, et al. A Review of the Potential Impacts of Climate Change on Bulk Power System Planning and Operations in the United States. Renew Sustain Energy Rev 2018;98:255–67. https://doi.org/10.1016/j.rser.2018.09.022.

[10] EIA. Electric Power Monthly 2017. https://www.eia.gov/electricity/monthly/.

[11] Go RS, Munoz FD, Watson JP. Assessing the Economic Value of Co-Optimized Grid-Scale Energy Storage Investments in Supporting High Renewable Portfolio Standards. Appl Energy 2016;183:902–13. https://doi.org/10.1016/j.apenergy.2016.08.134.

[12] Denholm P, Sioshansi R. The Value of Compressed Air Energy Storage with Wind in Transmission-Constrained Electric Power Systems. Energy Policy 2009;37:3149–58. https://doi.org/10.1016/j.enpol.2009.04.002.

[13] Buscheck T, Bielicki J, Edmunds T, Hao Y, Sun Y, Randolph J, et al. Multi-Fluid Geo-Energy Systems: Using Geologic CO_2 Storage for Geothermal Energy Production and Grid-Scale Energy Storage in Sedimentary Basins. Geosphere 2016;12. https://doi.org/10.1130/GES01207.1.

[14] Randolph JB, Saar MO. Combining Geothermal Energy Capture With Geologic Carbon Dioxide Sequestration. Geophys Res Lett 2011;38:1–7. https://doi.org/10.1029/2011GL047265.

[15] Saar MO, Randolph JB, Kuehn TH, the Regents of the University of Minnesota. Carbon dioxide-based geothermal energy generation systems and methods related thereto. U.S. Patent No. 8316955 (issued 2012); Canada Patent No. 2.753.393 (issued 2013); Europe Patent No. 2406562 (issued 2014); Australia Patent No. 2010223059 (issued 2015), n.d.

[16] Adams BM, Kuehn TH, Bielicki JM, Randolph JB, Saar MO. A Comparison of Electric Power Output of CO_2 Plume Geothermal (CPG) and Brine Geothermal Systems for Varying Reservoir Conditions. Appl Energy 2015;140:365–77. https://doi.org/10.1016/j.apenergy.2014.11.043.

[17] Adams BM, Kuehn TH, Bielicki JM, Randolph JB, Saar MO. On the Importance of the Thermosiphon Effect in CPG (CO_2 Plume Geothermal) Power Systems. Energy 2014;69:409–18. https://doi.org/10.1016/j.energy.2014.03.032.

[18] Garapati N, Randolph JB, Saar MO. Brine Displacement by CO_2, Energy Extraction Rates, and Lifespan of a CO_2-Limited CO_2-Plume Geothermal (CPG) System with Horizontal Production Well. Geothermics 2015;55:182–94. https://doi.org/10.1016/j.geothermics.2015.02.005.

[19] Buscheck TA, Sun Y, Chen M, Hao Y, Wolery TJ, Bourcier WL, et al. Active CO_2 Reservoir Management for Carbon Storage: Analysis of Operational Strategies to Relieve Pressure Buildup and Improve Injectivity. Int J Greenh Gas Control 2012;6:230–45. https://doi.org/10.1016/j.ijggc.2011.11.007.

[20] Buscheck TA, Bielicki JM, Randolph JB. CO_2 Earth Storage: Enhanced Geothermal Energy and Water Recovery and Energy Storage. Energy Procedia 2017;114:6870–9. https://doi.org/10.1016/j.egypro.2017.03.1615.

[21] Buscheck TA, White JA, Carroll SA, Bielicki JM, Aines RD. Managing Geologic CO_2 Storage with Pre-Injection Brine Production: A Strategy Evaluated with a Model of CO_2 Injection at Snøhvit. Energy Environ Sci 2016;9:1504–12. https://doi.org/10.1039/C5EE03648H.

[22] Deng H, Bielicki JM, Oppenheimer M, Fitts JP, Peters CA. Leakage risks of Geologic CO2 Storage and the Impacts on the Global Energy System and Climate Change Mitigation; 2017:151–63. doi:10.1007/s10584-017-2035-8.

[23] Bielicki M, Pollak MF, Deng H, Wilson EJ, Fitts P, Peters CA. The Leakage Risk Monetization Model for Geologic CO2 Storage; 2016. doi:10.1021/acs.est.5b05329.

[24] NETL. Carbon Storage Atlas - Fifth Edition (Atlas V); 2015.

[25] Coleman JL, Cahan SM. Preliminary Catalog of the Sedimentary Basins of the United States. US Geol Surv Open-File Rep 2012-111; 2012.

[26] Ogland-Hand JD, Bielicki JM, Wang Y, Adams BM, Buscheck TA, Saar MO. The Value of Bulk Energy Storage for Reducing CO_2 Emissions and Water Requirements from Regional Electricity Systems. Energy Convers Manag 2019;181:674–85. https://doi.org/10.1016/j.enconman.2018.12.019.

[27] Günter N, Marinopoulos A. Energy Storage for Grid Services and Applications: Classification, Market Review, Metrics, and Methodology for Evaluation of Deployment Cases. J Energy Storage 2016;8:226–34. https://doi.org/10.1016/j.est.2016.08.011.

[28] Paine N, Homans FR, Pollak M, Bielicki JM, Wilson EJ. Why Market Rules Matter: Optimizing Pumped Hydroelectric Storage when Compensation Rules Differ. Energy Econ 2014;46:10–9. https://doi.org/10.1016/j.eneco.2014.08.017.

[29] EPRI. Electricity Energy Storage Technology Options 2010. https://www.epri.com/#/pages/product/1022261/?lang=en-US.

[30] Sioshansi R, Denholm P, Jenkin T. Market and Policy Barriers to Deployment of Energy Storage. Econ Energy Environ Policy 2012;1:1–14. https://doi.org/10.5547/2160-5890.1.2.4.

[31] Sioshansi R, Denholm P, Jenkin T, Weiss J. Estimating the Value of Electricity Storage in PJM: Arbitrage and Some Welfare Effects. Energy Econ 2009;31:269–77. https://doi.org/10.1016/j.eneco.2008.10.005.

[32] Mines GL. GETEM User Manual 2016. https://workingincaes.inl.gov/SiteAssets/CAES Files/FORGE/inl_ext-16-38751 GETEM User Manual Final.pdf.

[33] U.S. DOE. GETEM: Geothermal Energy Technology Evaluation Model 2012. https://www.energy.gov/eere/geothermal/geothermal-electricity-technology-evaluation-model.

[34] EPA. Geologic CO2 Sequestration Technology and Cost Analysis; 2010.

[35] Moisseytsev A, Sienicki JJ. Investigation of a Dry Air Cooling Option for an SCO2 cycle. 4th Int Symp - Supercrit CO2 Power Cycles 2014;1:1–21.

[36] Pidaparti SR, Moisseytsev A, Sienicki JJ, Ranjan D. Counter Flow Induced Draft Cooling Tower Option for Supercritical Carbon Dioxide Brayton Cycle. Nucl Eng Des 2015;295:549–58. https://doi.org/10.1016/j.nucengdes.2015.09.026.

[37] Short W, Sullivan P, Mai T, Mowers M, Uriarte C, Blair N, et al. Regional Energy Deployment System (ReEDS); 2011. doi:NREL/TP-6A20-46534.

[38] NETL. Cost Estimation Methodology for NETL Assessments of Power Plant Performance. Quality Guidelines for Energy System Studies; 2011.

[39] Saar M, Randolph J, Adams B, Ogland-Hand J, Fleming M, Hefny M, et al. CCU3S: Combining CO2 Capture and Geologic Storage with: U1) Geothermal Power Generation, U2) Subsurface Grid-Scale Energy Storage, and U3) Cold Supply. KAUST Res Conf Matur Geotherm Energy Saudi Arab 2020.

[40] Hao Y, Sun Y, Nitao JJ. Overview of NUFT: A versatile numerical model for simulating flow and reactive transport in porous media. In: Zhang F, Yeh G, Parker JC, editors. Groundw. React. Transp. Model., Bentham Science; 2012, p. 213–40.

[41] USGS. National Assessment of Geologic Carbon Dioxide Storage Resources - Data (ver 1.1, Sept. 2013): U.S. Geological Survey Data Series 774. 2013.

[42] Frezon S, Finn T, Lister J. Total Thickness of Sedimentary Rocks in the Conterminous United States; 1983.

[43] Fuis G, Ryberg T, Godfrey N, Okaya D, Murphy J. Crustal Structure and Tectonics from the Los Angeles Basin to the Mojave Desert, Southern California. Geology; 2001: 29.

[44] Jachens R, Griscom A, Roberts C. Maps of the Thickness of Cenozoic Deposits and the Isostatic Residual Gravity over Basement for Nevada; 1996.

[45] Langenheim V, Jachens R. Gravity Data Collected Along the Los Angeles Regional Seismic Experiment (LARSE) and Preliminary Model of Regional Density Variations in Basement Rocks, Southern California; 1996.

[46] Mooney WD, Kaban MK. The North American Upper Mantle: Density, Composition, and Evolution. J Geophys Res Solid Earth 2010;115:1–24. https://doi.org/10.1029/2010JB000866.

[47] USGS. National Assessment of Geologic Carbon Dioxide Storage Resources - Results: U.S. Geological Survey Circular 1386; 2013.

[48] Jachens RC, Griscom A, Roberts CW. Regional Extent of Great Valley Basement West of the Great Valley, California: Implications for Extensive Tectonic Wedging in the California Coast Ranges. J Geophys Res 1995;100:12769. https://doi.org/10.1029/95JB00718.

[49] EIA. Frequently Asked Questions: How Much Carbon Dioxide is Produced Per Kilowatthour of U.S. Electricity Generation? 2019. https://www.eia.gov/tools/faqs/faq.php?id=74&t=11.

[50] EPA. Inventory of U.S. Greenhouse Gas Emissions and Sinks 2019. https://www.epa.gov/ghgemissions/inventory-us-greenhouse-gas-emissions-and-sinks.

[51] NREL. Development of Regional Wind Resource and Wind Plant Output Datasets: Final Subcontract Report 15 October 2007 - 15 March 2009; 2010. https://www.nrel.gov/docs/fy10osti/47676.pdf.

[52] USGS. Energy News and Current Publications 2013.

[53] Draxl C, Clifton A, Hodge BM, McCaa J. The Wind Integration National Dataset (WIND) Toolkit. Appl Energy 2015;151:355–66. https://doi.org/10.1016/j.apenergy.2015.03.121.
[54] CAISO. Locational Marginal Prices. OASIS n.d.
[55] Eichman J, Denholm P, Jorgenson J. Operational Benefits of Meeting California's Energy Storage Targets; 2015. https://www.nrel.gov/docs/fy16osti/65061.pdf.
[56] CAISO. Integration of Renewable Resources: Technical Appendices for California ISO Renewable Integration Studies. Version 1, First Draft for External Review; 2010.
[57] IPCC. IPCC Special Report on Carbon Dioxide Capture and Storage. 2005. doi: 10.1557/mrs2008.6.
[58] Fleming MR, Adams BM, Randolph JB, Ogland-Hand JD, Kuehn TH, Buscheck TA, et al. High Efficiency and Large-Scale Subsurface Energy Storage with CO2. 43rd Stanford Work Geotherm Reserv Eng 2018:1–12. https://pangea.stanford.edu/ERE/pdf/IGAstandard/SGW/2018/Fleming.pdf.
[59] Ogland-Hand JD, Miranda MW, Bielicki JM, Adams BM, Buscheck TA, Saar MO. Operational Characteristics of a Geologic CO_2 Storage Bulk Energy Storage Technology. Energy Procedia 2018.
[60] Climate Policy Initiation. California Carbon Dashboard; 2017.
[61] EIA. Regional Greenhouse Gas Initiative Auction Prices are the Lowest Since 2014. Today In Energy 2017. https://www.eia.gov/todayinenergy/detail.php?id=31432.
[62] IRC. §45Q: Credit for Carbon Oxide Sequestration 2019;43:1–6. https://uscode.house.gov/view.xhtml?req=(title:26 section:45Q edition:prelim).
[63] EPA. The Social Cost of Carbon 2017. https://19january2017snapshot.epa.gov/climatechange/social-cost-carbon_.html.